Vorticity component distributions in the near field of a wall jet

Thrassos Panidis[2], Andrew Pollard[1*] and Rainer Schwab[1]
[*]Author for correspondence
[1]Department of Mechanical and Materials Engineering, Queen's University, Kingston, Canada
[2]Mechanical Engineering and Aeronautics Department, University of Patras, Patras, Greece
Email: pollarda@queensu.ca, panidis@mech.upatras.gr

ABSTRACT

Experimental results on the near field development of a turbulent rectangular wall jet with aspect ratio 10, issuing from a sharp-edged orifice at $Re_h \sim 23{,}000$ are presented and discussed. Hot wire X-probe measurements on cross plane grids provide information on the 3D characteristics of the flow field. Mean vorticity components were estimated by interpolation and derivation from the mean velocity measurements. Contour plots of flow characteristics are presented and discussed to uncover some complex flow physics.

NOMENCLATURE

h	[m]	Wall jet slot height
U	[m/s]	Axial mean velocity
V	[m/s]	Spanwise mean velocity
W	[m/s]	Lateral (wall normal) mean velocity
x	[m]	Cartesian axis direction
y	[m]	Cartesian spanwise axis direction
z	[m]	Cartesian lateral (wall normal) axis direction

Special characters

Ω_X	[1/s]	Vorticity in axial direction
Ω_Y	[1/s]	Vorticity in spanwise direction
Ω_Z	[1/s]	Vorticity in lateral direction

Subscripts

cl	centreline
max	Maximum

INTRODUCTION

Features unique to the free jet flow from sharp-edged orifices are the development of a vena contracta in the plane of the major axis of the jet (the spanwise direction) and the formation of saddle-backed velocity profiles in the characteristic decay region (typically, $5 < x/h < 30$, where x is the streamwise coordinate direction and h is the slot height). The off-centre velocity peaks have been found to vary in magnitude depending on the jet aspect ratio and inlet conditions, but more importantly, for the present configuration, Vouros et al. [1] noted that "two key features of this type of jet are mean axial velocity profiles presenting two off axis peaks, commonly mentioned as saddleback profiles, and a predominant dumbbell shape as described by, for example, a contour of the axial mean velocity. The saddleback shape is found to be significantly influenced by the vorticity distribution in the transverse plane of the jet, while the dumbbell is traced to two terms in the axial mean vorticity transport equation that diffuse fluid from the centre of the jet towards its periphery."

In the case of wall jets that issue from a rectangular nozzle, the spread rate in the wall normal and wall spanwise direction is anisotropic, see Launder and Rodi [2] with that in the spanwise exceeding that in the wall normal direction. There have been numerous investigations to explain the cause of this anisotropic spreading. Craft and Launder [3] suggest that the larger lateral spreading of the wall jet is due to the "creation of streamwise vorticity". Moreover, they note that the "predicted ratio of the (wall) normal to lateral spreading rates is, however, very sensitive to the approximation made for the pressure-strain correlation". Hall and Ewing [4] suggest "Contours of the full flow field indicate that the turbulent mechanism that causes the lateral growth of the three-dimensional wall jets is located in the lateral shear layers near the wall". However, they provided no direct evidence of what maybe physically occurring in those shear layers, such as vorticity distributions.

In this paper, the 10:1 aspect ratio free jet, explored originally by Schwab [5], Pollard and Schwab [6] and those data being reinterpreted by Vouros et al. [1], is moved such that the flow issues parallel to a flat wall. These wall jet data are reinterpreted by reference to the mean vorticity components and the streamwise vorticity budget equation to delineate the role of vorticity to the development of specific characteristics in the flow development.

EXPERIMENTAL CONDITIONS

The air jet was produced by a sharp-edged rectangular orifice of dimensions 70x7 mm^2 (equivalent hydraulic diameter $D_h = 12.73\ mm$) mounted on the downstream end of a 1.05 m long, square cross sectioned settling chamber 0.350 *m* to the side. The exit Reynolds number, based on the slot height (h=7mm) and jet exit velocity, U_{exit}, was $Re_h = 23{,}000$. Measurements were carried out using a constant temperature anemometer and a miniature X wire probe. The velocity components in the streamwise (x-axis) and the spanwise (y-axis, parallel to the long side of the orifice) directions were measured and upon probe rotation the vertical velocity components were obtained (z-axis). Data were collected at equally spaced positions on cross plane grids at x/h= 1, 2, 3, 5, 7, 10, 15 and 20 from jet exit, see Schwab [5] for further

details. The origin of the Cartesian coordinate system used in this work is located on the intersection of the wall plane and the short central axis of the orifice on the jet exit plane, see Figure 1.

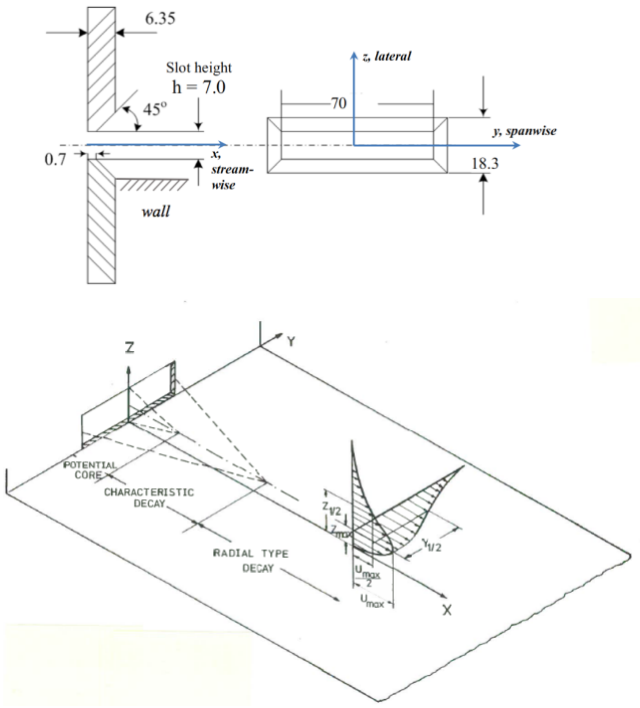

Figure 1 Chamfered rectangular orifice. Wall is located parallel to and coincident with the lower spanwise edge. Note that all plots use wall as origin for lateral direction (z/h=0 on wall). All units in mm. From Schwab [5].

PRESENTATION AND DISCUSSION OF RESULTS

It is to be recalled that in Vouros et al. [1], it was concluded that some of the main features of the rectangular jet can be traced back to the non-equal contraction rates experienced by the fluid as it approached the exit plane. The rectangular exit gave rise to four counter rotating vortices, one in each of the four quadrants of the jet. In particular, *with the observer facing upstream* (as in all figures presented here), these vortices rotate clockwise in the upper right and lower left corner and counter-clockwise in the lower right and upper left corner of the jet. Indeed, Vouros et al. [1] argued that these vortices played a significant role in the downstream development of the free jet, including contributing to the formation of both a "dumbbell" shaped cross section to the jet as well as to the well-known saddled-backed velocity profiles, see for example Sfeir [7] and others. As an aside, the asymmetry between the settling chamber and a rectangular shaped exit diminishes to zero as the jet aspect ratio returns to being the same as the settling chamber, thereby eliminating these vortices [1]. Thus, the current contribution can not be divorced from the flow physics and insight provided by Vouros et al. [1].

Flow Visualisation

We begin by presenting a flow visualisation of the flow taken at x/h=2 in Figure 2 [5]. This figure was obtained by injecting smoke into the settling chamber and passing a laser light sheet through a plane parallel to the jet exit at x/h=2. The picture illustrates a number of features that will be observed in the plots to be presented later.

The first point to note is the undulations along the upper surface of the jet. These are indicative of the "dumbbell" shape mentioned earlier. On the lower right, resting on the wall, is a "tuft" of fluid that appears as a circle. While it is difficult to discern, it can be inferred that this tuft rotates in a counter clockwise direction, suggesting that is a remnant from the settling chamber, as noted earlier. In this picture there does not appear to be a counter part in the upper right quadrant, but there is evidence of both on the left side of the jet.

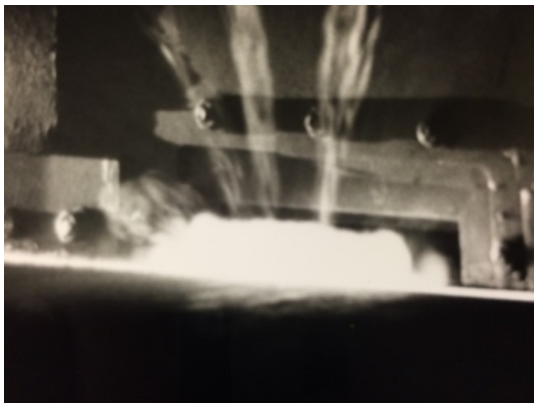

Figure 2 Visualisation of wall jet flow at x/h=2. Note smoke tuft on wall, right side of nozzle; and, undulation along top surface of jet. Vertical streaks of smoke indicate entrainment. From Schwab [5].

Figure 2 illustrates that the wall obviously impacts the lower portion of the jet as it develops into a wall jet, while the upper surface remains somewhat immune, at least based upon earlier findings of jet development observed by Schwab [5] and Vouros et al. [1].

Mean velocity contours

The data to be presented appear in their raw form in Schwab [5]. These data were digitised and derivative variables and contour plots presented herein have been produced by applying the 'inverse distance interpolation' scheme on the raw measurements using Tecplot™; for further information, see Vouros et al. [1]. In all plots, the two black contour lines indicate the locations where the mean streamwise velocity are equal to U/U_{cl}=0.5 and 0.95, where U_{cl} is the local centreline velocity. Note that the jet features a *vena-contracta*, such that the cross sectional area continues to diminish in size up to about x/h=1-2, before expanding again with increased downstream distance.

From Figure 3, it is apparent that the axial mean velocity displays a "dumbbell" shape that is symmetric about the lateral

centreline, while its symmetry about the spanwise centreline diminishes as the jet continues to be influenced by the wall as it evolves in the axial direction. Furthermore, two islands where U/U_{cl}=0.95 emerge at x/h=5 are apparent. These islands are the peaks in the saddle-backed velocity profiles (SBVP). Here, however, the peaks in the SBVP eventually coalesce at x/h=20. This coalescence occurs well before that location were the jet to freely evolve [1]. It maybe surmised that the wall enhances the spanwise diffusion to effect this outcome. The data further indicate a relatively higher spreading in the lateral direction resembling the axis switching of a free jet. Finally the attraction of the jet downstream towards the wall due to a Coanda effect has to be highlighted. The span and lateral mean velocity (V and W) contours (ignoring the colour changes in the plots that are around zero in magnitude) indicate symmetry about their respective axes but otherwise convey little of what will be claimed as complex flow physics in the near field of this flow.

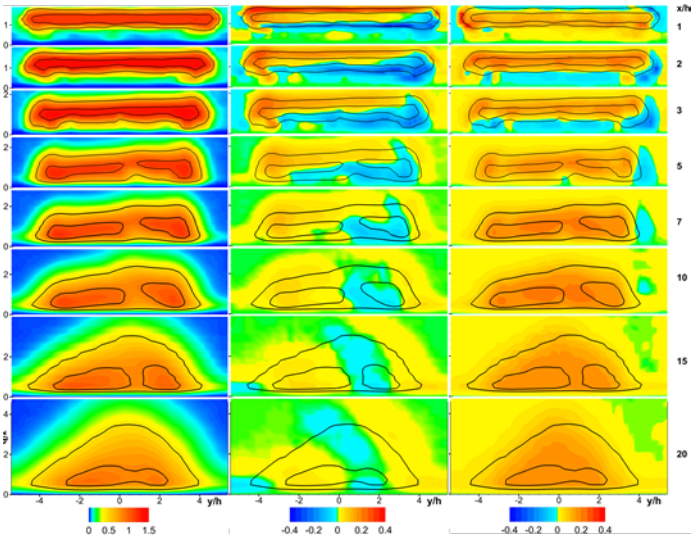

(a) U/U_{exit} (b) V/U_{exit} (c) W/U_{exit}

Figure 3 Mean velocity contours at x/h=1, 2, 3, 5, 7, 10, 15, 20. Note scale change for V/U_{exit} and W/U_{exit}

Turbulence Reynolds stress contours

The rms values of the Reynolds normal stresses will not be presented here; suffice it to say they display excellent symmetry about the lateral axis. The Reynolds shear stresses are plotted in Figure 4. From this Figure, the negative values (blue) of $\overline{uw}/U^2_{exit}$ between the wall and the jet mid-plane are seen to decrease with increased x/h, while the intensity of the positive values (reddish) similarly diminish.

The contours of vorticity

First, consider the vorticity magnitude, streamwise (X), spanwise (Y) and lateral (Z) vorticity as provided in Figure 5. Each vorticity is normalised using U_{exit}/h. When compared to similar plots for the free jet, marked differences are observed. In the first instance, attention is focussed on the vorticity magnitude, |Ω|, in Fig. 5. As mentioned earlier, the wall interferes with the symmetric development of the jet above and below the spanwise centreline; even so, considerably large values in vorticity magnitude emerge below the saddle-back peaks at about y/h=+/-4 (the red streaks at x/h=3, for example). The contours of Ω_X indicate that the flow retains the four corner vortices identified by Vouros et al. [1] such that the upper right quadrant fluid rotates clockwise and that below it rotates counter clockwise and opposite to those on the left side of the transverse symmetry plane. In the downstream field, after say x/h=7 a vortex system develops at the central area close to the wall as indicated by the arrows on the last station's plot.

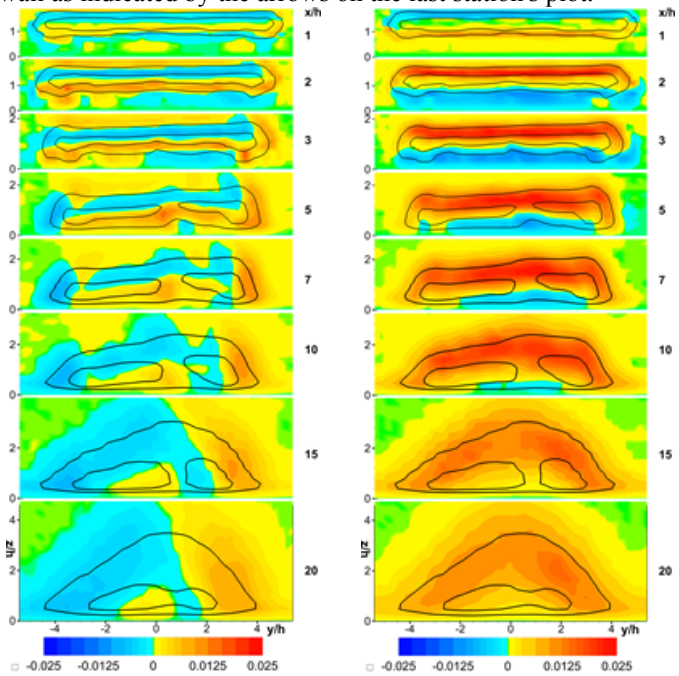

(a) $\overline{uv}/U^2_{exit}$ (b) $\overline{uw}/U^2_{exit}$

Figure 4 Reynolds shear stresses at x/h=1,2,3,5,7,10, 15 & 20.

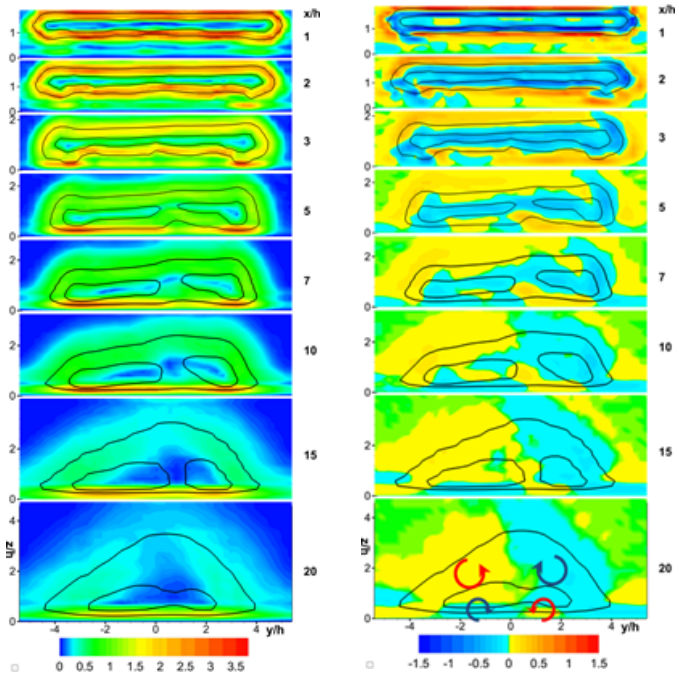

(a) $|\Omega|/(U_{exit}/h)$ (b) $\Omega_x/(U_{exit}/h)$

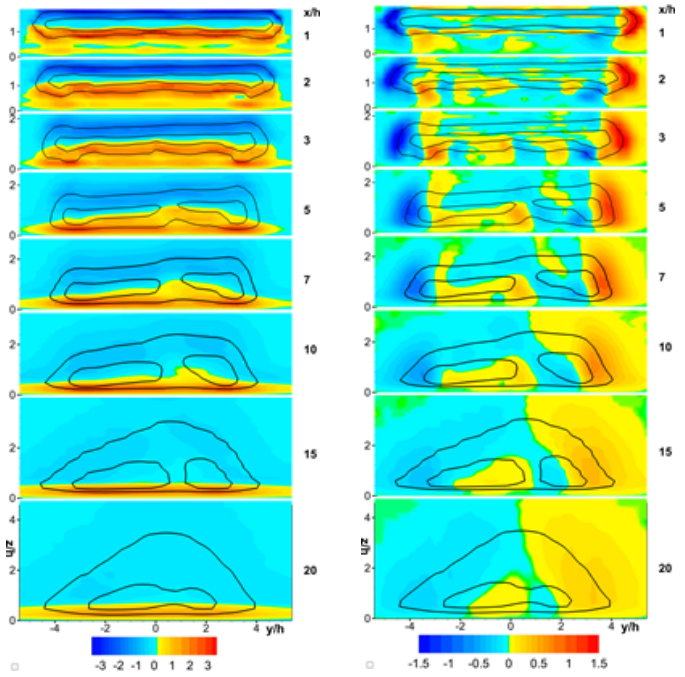

(c) $\Omega_y/(U_{exit}/h)$ (d) $\Omega_z/(U_{exit}/h)$

Figure 5 Contours of vorticity

The contours of Ω_Z in Figure 5, clearly identify that the sense of fluid rotation positive and negative on either side of the jet. This implies that the short sides of the jet must play a role in spanwise spreading of the jet. Taken alone, it may be argued that this vorticity engulfs free stream fluid which would cause the flow to diverge away from the centreline. The combination of Ω_Y and Ω_Z (note the difference in their magnitudes, with spanwise vorticity being larger than the lateral) suggests that the spanwise vorticity engulfs free stream fluid that would then, it is surmised, assist to feed the lateral spreading, at least in the near-field, say x/h < 5. Beyond that plane, the lateral vorticity approaches the magnitude of the spanwise along the jet free surface. The spanwise vorticity remains intense next to the wall, and indeed throughout the domain considered here.

The axial mean vorticity equation

The axial mean vorticity equation for turbulent flow is [2]:

$$\frac{D\Omega_X}{Dt} = \underbrace{\Omega_X \frac{\partial U}{\partial x}}_{A} + \underbrace{\Omega_Y \frac{\partial U}{\partial y}}_{B} + \underbrace{\Omega_Z \frac{\partial U}{\partial z}}_{C} + \underbrace{\frac{\partial^2}{\partial y \partial z}(\overline{w^2} - \overline{v^2}) + \frac{\partial^2}{\partial y^2}(\overline{vw}) - \frac{\partial^2}{\partial z^2}(\overline{vw})}_{D} + \underbrace{\nu\left(\frac{\partial^2 \Omega_x}{\partial y^2} + \frac{\partial^2 \Omega_x}{\partial z^2}\right)}_{E} \quad (1)$$

where the first three terms A, B and C on the RHS represent vorticity amplification or attenuation due to streamwise stretching and vortex-line bending, the next three terms, D, the contributions from the Reynolds stresses and, of course, E represents dissipation.

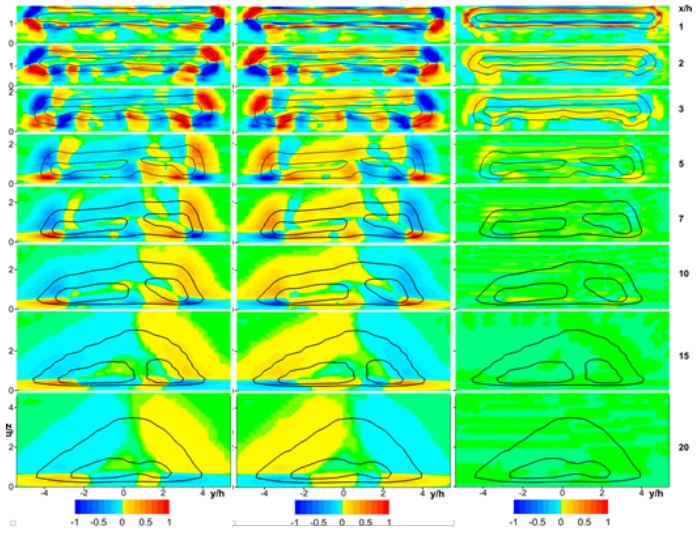

(α) Term B (b) Term C (c) Sum of Terms B & C

Figure 6 Contour plots of terms B, C and B+C of Equation (1).

These terms, B and C, have been chosen to highlight the important role of both the lateral and spanwise vorticity component in the mean axial vorticity equation. Some of the individual terms that comprise the vorticity field are displayed in the plots of Figure 6, where the right hand figure represents

$$\frac{\partial U}{\partial z}\frac{\partial V}{\partial x} - \frac{\partial W}{\partial x}\frac{\partial U}{\partial y} \quad (2)$$

after expansion of the terms B and C. From Equation (2), the gradients of U are more likely larger that their multiplicands, since the gradients of U in the wall normal (both positive and negative depending upon being below or above the axial velocity maximum) and spanwise directions (being symmetric about the lateral centreplane of the jet) with that of the first term being larger than the second.

As found in the free jet case, the B-term is positive in the upper right hand and negative in the lower corner, while the C-term is a reflection of these. With increased downstream distance from the nozzle exit plane, the upper right corner of the B-term overwhelms that of the lower right, at least in spanwise cross sectional area, which implies a diffusion of that portion of the vorticity. In the lower right portion, the intensity of the vorticity, while diminished in cross sectional area, remains rather intense. Since the B- and C-terms were suggested to be dominated by gradients in the axial velocity, it must be noted that gradients in axial mean velocity are greatest in the lateral direction, positive between the wall and U_{max} (see figure 1) and negative from there to the free stream.

The product of terms in B and C give rise to the positive and negative "islands" observed in Figure 6 for $1 < x/h < 7$, say. These are similar to those found in the free jet case, which were connected to the formation of the dumbbell shape and the saddle backed velocity profiles. A significant feature of these terms is the emergence of positive and negative regions at $x/h > 10$. There are three areas: the positive and negative areas that are inclined at approximately 30 degrees at $x/h = 15$ and approximately 45 degrees at $x/h = 20$ to the horizontal and above the lateral location where $U=U_{max}$, and another region between there and the wall. While data are available for $x/h > 20$ (Schwab and Pollard [8]), they have yet to be processed in the manner presented here, so that the inclination of the regions may change further with increasing x/h. From the vorticity plots of Figure 5 it seems that Ω_Z contributes more to these inclined regions than Ω_Y, but the terms B and C provide equal, but opposite contributions such that they cancel as can be observed from the sum of the terms B and C. This probably indicates that, at least for the sharp edged, high aspect ratio jet, the development of the streamwise vorticity distribution is rather weakly affected by the combined effect of the terms B and C as postulated in the analysis of Launder and Rodi [2].

CONCLUSION

The use of computer interpolation techniques on available 3D experimental measurements are used to further exploit previously available velocity data, which provide information on the vorticity distributions in a turbulent rectangular wall jet. The development of the sharp edged jet of aspect ratio 10 is characterized by a mean velocity distribution with a predominantly "dumbbell" outline, presenting two off centre peaks similar to the saddle back profile of the free jet and a relatively higher spreading in the vertical direction away from the wall resembling the axis switching of a free jet. A third further characteristic, unique to the wall jet, is the attraction of the jet downstream, towards the wall due to a Coanda effect. The streamwise vorticity component indicate, at downstream locations, a system of four vortices in the central area of the wall jet, whereas the transverse components are mostly dictated by the streamwise velocity gradients across the shear layers developing around velocity peaks. At the farthest downstream locations, the spanwise vorticity component close to the wall becomes dominant due to the wall shear layer. The streamwise vorticity seems to significantly affect the development of the jet. The presented terms of the longitudinal vorticity budget provide insight regarding the interaction of the jet flow structures although their contribution does not seem sufficient to fully explain the role of vorticity in flow development.

ACKNOWLEDGEMENTS

AP and RRS acknowledge the Natural Sciences and Engineering Research Council of Canada and Queen's University for funding the original work and for continued support to AP. TP acknowledges the support of the University of Patras. Both AP and TP appreciate the support of the Mechanical Engineering and Aeronautics Department of the university of Patras for hosting AP during a recent sabbatical. We also acknowledge the diligent efforts of Mr. Giuseppe Garro for the many hours spent to digitize the data from the hard copy contained in Dr. Schwab's thesis.

REFERENCES

[1] Vouros A., Panidis T., Pollard A. and Schwab R., Near field vorticity distributions from a sharp-edged rectangular jet, *International Journal of Heat and Fluid Flow*, Vol. 51, 2015, pp. 383-394

[2] Launder B.E. and Rodi W., The turbulent wall jet – Measurements and modelling, *Annual Review of Fluid Mechanics,* Vol. 15, 1983, pp. 429-459.

[3] Craft T.J. and Launder B.E., On the spreading mechanism of the three dimensional wall jet, *Journal of Fluid Mechanics*, vol. 435, 2001, pp 305-326

[4] Hall J. W. and Ewing D., Three-dimensional turbulent wall jets issuing from moderate-aspect-ratio rectangular channels, AIAA Journal, Vol. 45, No. 6, 2007, pp. 1177-1186

[5] Schwab R.R., An experimental and numerical investigation of three-dimensional jet flows from sharp-edged orifices, *Ph.D. thesis, Queen's University at Kingston,* 1986

[6] Pollard A. and Schwab R.R., The near field behaviour of rectangular free jets: An experimental and numerical study, *Proceedings, First world conference on experimental heat transfer, fluid mechanics and thermodynamics*, Dubrovnik, Croatia, pp 1510-1517, 1988

[7] Sfeir A., Investigation of three-dimensional turbulent Rectangular jets, *AIAA Journal*, Vol. 17, No. 10, 1979, pp. 1055–1060

[8] Schwab R.R. and Pollard A., An Experimental Investigation of Wall Jets Issuing from Rectangular Sharp-Edged Orifices, *Proceedings, 7th Symposium on Turbulent Shear Flows*, Stanford University, Stanford, California, 1989